9th International IEEE EMBS Conference on Neural Engineering
San Francisco, CA, USA, March 20 - 23 , 2019

Dynamic Modeling and Classification of Epileptic EEG Data*

Xiaomu Song[1,3], Luis Aguilar[2], Angela Herb[3], and Suk-chung Yoon[4]

***Abstract*— Brain functional connectivity has been used to investigate the interaction between brain regions. It provides important information related to brain diseases, injuries, and high level cognitive functions. Statistical methods have been widely used to model brain functional connectivity based upon which insights of brain function are expected to be revealed. Most statistical approaches were developed based upon an assumption that connectivity patterns are static during the recording. This is not true because the connectivity changes over time. A dynamical modeling of connectivity patterns allows to characterize these variations. In this work, a simplified dynamic Bayesian modeling approach, parallel Hidden Markov Model (PaHMM), was investigated by characterizing temporal variations of cortical functional connectivity patterns computed using epileptic electroencephalogram (EEG) data. The performance of the PaHMM was evaluated based on an experimental study of epilepsy detection and classification, where multisubject epileptic EEG data from Temple University Hospital EEG Data Corpus were used. Experimental results show that an accuracy of 93.5% was obtained for the epilepsy detection, and an overall accuracy above 81% was achieved for the seizure type classification. This indicates that the method can efficiently capture temporal variations of functional connectivity patterns, and is potentially applicable in clinical settings to detect epilepsy and differentiate seizure types.**

I. INTRODUCTION

Epilepsy is a neurological disorder that causes recurring seizures. According to World Health Organization, there are approximately 50 million people (about 0.6–0.8% of the worlds population) who have active epilepsy [1]. Electroencephalogram (EEG), a noninvasive electrophysiological monitoring technique that can record brain electrical activity by electrodes placed on the scalp, has been intensively used for the diagnosis of epilepsy within last many years. A typical diagnostic EEG scanning for epilepsy detection takes from multiple days up to several weeks. In most hospitals and clinic offices, the EEG recordings are visually inspected by trained medical staff. This procedure is time-consuming, and misdiagnosis rate is usually high [2].

There have been efforts to develop automatic EEG-based epilepsy detection and classification techniques [3], [4], [5], [6]. Within these studies, different features have been investigated for EEG classification, such as band power, spectral entropy, autoregressive parameters, complexity stochastic measure, and Hjorth parameters [5]. In this work, we investigate the feasibility of using cortical functional connectivity calculated from EEG data as a feature for the detection and classification of epilepsy.

Brain functional connectivity has been widely investigated in neuroscience fields with potential clinical applications, such as early diagnosis of neurodegenerative diseases [7]. The traditional approach to quantify functional connectivity is based upon the assumption that connectivity patterns do not change during each trial of EEG recording, which is not true. In recent years, more studies have been focused on the modeling of changes of functional connectivity, which are expected to provide better characterization of brain functional networks [8], [9]. Dynamic Bayesian network (DBN) is one of dynamic modeling methods that can be used to characterize changes of functional connectivity [10]. In this work, a simplified DBN model is used to quantify dynamic changes of multiple cortical functional connectivity patterns [11]. Clinic epilepsy EEG data from the Temple University Hospital EEG Data Corpus were used in the experimental study to evaluate the model performance for the detection and classification of epilepsy [12].

The remaining of the paper is organized as follows. An introduction to DBN is provided in section II. In section III, epileptic EEG data used in this study are described. The details of our method is elaborated in section IV, and experimental results are presented in section V, followed by the conclusion section.

II. DYNAMIC BAYESIAN NETWORK AND HIDDEN MARKOV MODEL

DBN is a graphic model that can be used to characterize a system that is dynamically change over time [13]. Even though there is a "dynamic" in the model's name, DBN itself does not change over time but is used to model dynamic changes [13]. Let $\mathbf{X}_{1:T} = \{\mathbf{X}_t, t = 1, 2, \cdots, T\}$ be a time series collected at T time points, if we assume the dynamic change within the time series to be a first-order Markovian, then the joint probability of all $\mathbf{X}_t$ is:

$$P(\mathbf{X}_{1:T}) = P(\mathbf{X}_1) \prod_{t=2}^{T} P(\mathbf{X}_t | \mathbf{X}_{t-1}). \quad (1)$$

When DBN is applied to model brain functional networks, the model learning usually involves model structure learning and parameter estimation [9]. Typically $\mathbf{X}_t$ is a vector consisting of N observations $\mathbf{X}_t = \{x_t^n, n = 1, 2, \cdots, N\}$ corresponding to N regions of interest (ROI) in each time slice. The observation in each ROI could be its average time course or any other measures that carry functional variations across time.

*This work was supported by Widener University Faculty Development Option Grant.

[1]Robotics Engineering Department, [2]Biomedical Engineering Department, [3]Electrical Engineering Department, School of Engineering, Widener University, Chester, PA 19013

[4]Computer Science Department, College of Arts and Sciences, Widener University, Chester, PA 19013

978-1-5386-7921-0/19/$31.00 ©2019 IEEE

In this work, DBN is used to model the dynamic changes of functional connectivity. In order to reduce computational load, instead of learning a network structure of all possible functional connectivity, we assume the connectivity pattern is known a priori, and DBN is directly used to model temporal variations of functional connectivities for pre-selected ROI pairs. As a result, only model parameters need to be estimated. Assume that there are M pairs of ROIs, and let $\mathbf{X}_t = \{x_t^1, x_t^2, \cdots, x_t^M\}$ be the connectivity measures of these ROI pairs at time t. Each connectivity measure is calculated between a pair of ROIs. If we assume that the observed connectivity measures $\mathbf{X}_{1:T}$ are generated by a process whose states are hidden $\mathbf{S}_{1:T} = \{\mathbf{S}_t, t = 1, 2, \cdots, T\}$, then the joint probability of all connectivity measures and associated hidden states is represented as:

$$P(\mathbf{X}_{1:T}, \mathbf{S}_{1:T}) = P(\mathbf{S}_1)P(\mathbf{X}_1|\mathbf{S}_1)\prod_{t=2}^{T} P(\mathbf{X}_t|\mathbf{S}_t)P(\mathbf{S}_t|\mathbf{S}_{t-1}), \quad (2)$$

where $\mathbf{S}_t = \{s_t^m, m = 1, 2, \cdots, M\}$ represents the hidden states of all connectivity measures in $\mathbf{X}_t$. If we further assume that the hidden state variable $\mathbf{S}_t$ is discrete, and the variations of the hidden states are first-order Markovian, then the DBN model becomes a hidden Markov model (HMM), as shown in Fig. 1, where each clear node represents all connectivity measures observed at time t, the connected shaded node indicates the hidden states, and the edges connecting the shaded nodes represent the evolution of time and the first-order Markov chain.

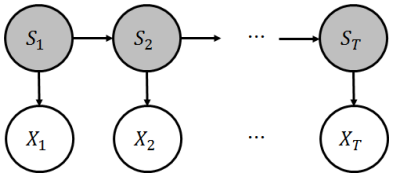

Fig. 1. Hidden Markov model.

In Fig. 1, the observation $\mathbf{X}_t$ contains M connectivity measures. If the hidden states of these connectivity measures are assumed to be independent to each other, then the original HMM can be simplified to a parallel HMM (PaHMM) [11]. Fig. 2 illustrates the structure of PaHMM for the dynamic modeling of the $m-1^{th}$ and m^{th} functional connectivity measures. The learning of a DBN model structure is computationally demanding where Markov Chain Monte Carlo simulation is often used [10], [14]. Compared to the DBN learning, the learning of a PaHMM is computationally much less expensive because no model structure learning is required, and the model parameter estimation is performed within each Markov chain.

III. Experimental Data

The experimental data were obtained from the Temple University Hospital EEG Corpus (TUH-EEG database) [12].

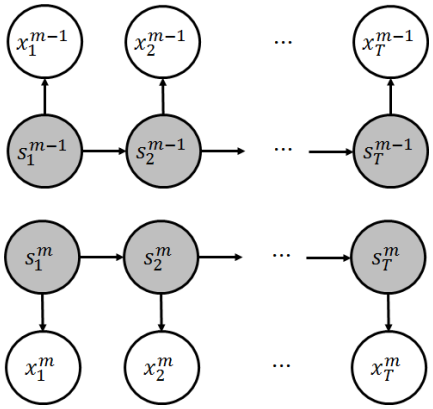

Fig. 2. Parallel hidden Markov model.

This database consists of over 16,000 sessions of EEG recordings acquired from more than 10,000 subjects. The ages of these subjects range from one year to over ninety years' old. 51% of subjects are female and 49% are male. A subset of EEG data collected from 124 subjects with epilepsy were used in this study, along with another subset of data collected from 7 healthy subjects that were used as the control group data. These data were sampled at a rate of 250Hz, and the time points when a seizure starts and ends in each trial are provided by the database. Based upon the time information, in each trial two seconds' recording were extracted for the analysis: one second before the seizure starts, and one second after the seizure starts, resulting in 500 samples in each trial. A small amount of EEG trials were collected using a headset that is different to the one used for acquiring the other trials. As a result, the number of EEG channels is not consistent across all trials. To solve this issue, the common EEG channels from these data were chosen, results in a total of 21 EEG channels for each trial. Based on these common EEG channels, 14 functional ROIs were selected for the analysis. Table I lists all of these ROIs, their corresponding Brodmann areas, and the associated EEG channels.

TABLE I
Functional regions, associated Brodmann areas and EEG channels.

Functional Region	Brodmann Area	EEG Channel
Executive Functions L	10L	Fp1
Executive Functions R	10R	Fp2
Motor Functions L	8L	F3
Motor Functions R	8R	F4
Somatosensory L	2L	C3
Somatosensory R	1R	C4
Attention L	39L	P3
Attention R	39R	P4
Visual L	18L	O1
Visual R	18R	O2
Executive Functions L	47L	F7
Executive Functions R	47R	F8
Sound L	42L	T3
Sound R	42R	T4
Memory L	20L	T5
Memory R	20R	T6

IV. Method

Both PaHMM-based epilepsy detection and classification were investigated using the experimental EEG data. In the study of epilepsy detection, 100 trials data from 25 patients with epilepsy and 100 trials from the 7 healthy subjects in the control group were used to train a PaHMM. The evaluation data consists of the same numbers of trials from the same patient and control groups. All training and evaluation data from the patients were acquired when there was no seizure occurring. For epilepsy classification, 144 trials data from 99 patients were used for the PaHMM model training, and another 144 trials from the same patient group were used for the evaluation. All patient training and evaluation data were collected when seizures occurred. There are seven different types of epileptic seizures in these trials, including: Focal Non-Specific Seizure (FNSS), Generalized Non-Specific Seizure (GNSS), Simple Partial Seizure (SPS), Complex Partial Seizure (CPS), Absence Seizure (AS), Tonic Seizure (TS), and Tonic Clonic Seizure (TCS). Table II lists the number of trials and the number of patients in each seizure type. The training and evaluation trials are from the same subjects for each type of seizure.

TABLE II
EXPERIMENTAL DATA OF SEVEN TYPES OF EPILEPTIC SEIZURES. THE NUMBERS OF TRAINING AND EVALUATION TRIALS ARE THE SAME IN EACH TYPE OF SEIZURE.

Seizure Type	No. of Trials	No. of Subjects
Focal Non-Specific Seizure	25	25
Generalized Non-Specific Seizure	25	25
Simple Partial Seizure	24	2
Complex Partial Seizure	25	25
Absence Seizure	25	11
Tonic Seizure	8	1
Tonic Clonic Seizure	12	10

Based on the 14 functional ROIs shown in Table I, there are a total of 91 connections, corresponding to 91 ROI pairs. To obtain dynamic variations of these connections, a sliding time window is used to divide EEG time series into multiple segments, each of which consists of 100 sample points. In this process, the sliding window is shifted each time by a fixed number of sample points, which also determines the amount of overlap between successive segments. Pearson's correlation coefficient (cc) is computed between two 100-sample data segments from two ROIs within the same time window to quantify the functional connectivity between them. The Fisher r-to-z transformation is performed to make the computed cc values to be approximately normally distributed [15]:

$$z = 0.5 * \ln \frac{1+r}{1-r}, \tag{3}$$

where r is the original cc value ranged between -1.0 and 1.0, and z is the transformed cc value. When calculating the cc value between two ROIs, the data acquired from the EEG channel located in each ROI are used as the representative temporal profile of this ROI. If there are more than one EEG channels in an ROI, the average of these channels is calculated as the representative temporal profile for the ROI.

For each functional connection, after calculating the normalized cc values using the time-shifted data segments, a PaHMM is constructed to dynamically model the temporal variations of these normalized cc values for all 91 connections. In this work, two hidden states are defined for the PaHMM. One is "connected", indicating a functional connection. The other is "unconnected", denoting no functional connectivity. The expectation maximization (EM) algorithm is used to estimate the model parameters. After the model estimation, the maximum likelihood (ML) criterion is used to make the final decision.

The epilepsy detection is a two-class classification problem where the EEG data are used to classify the subjects into two groups:"with epilepsy" and "without epilepsy". Three numerical criteria are used for the detection: accuracy, precision, and recall. Accuracy is the percentage of subjects that are correctly classified as "with epilepsy" and "without epilepsy". Precision is the percentage of subjects classified as "with epilepsy" are truly with epilepsy. Recall is the percentage of subjects with epilepsy that can be classified as "with epilepsy". For the seizure classification, the overall accuracy is used. In addition, different time shifts between successive segments may lead to different characterizations of temporal changes of functional connectivity, and affect the epilepsy detection/classification performance. This was investigated in this work, and the findings are reported and discussed in the following section.

V. Results

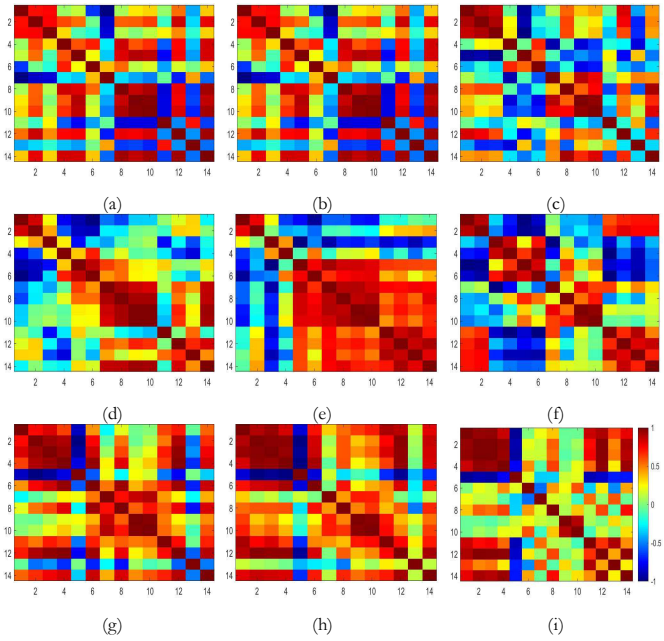

Fig. 3. The time-varying functional connectivity patterns of a single patient with epilepsy. Each connectivity is quantified by the cc value of the corresponding ROI pair. (a) cc map generated by the first 100-sample segments from the temporal profiles of the 14 ROIs. (b)-(i) cc maps obtained after shifting the time window by 50 samples each time. The cc map in (f) shows the moment right after a Focal Non-Specific seizure occurred.

Fig. 3 shows an example of time-varying cc maps obtained using a patient's data when a Focal Non-Specific seizure occurred. Fig. 3 (a) is the cc map computed using the first 100-sample segments from the 14 ROIs. (b) is the cc map using the second 100-sample segments that were generated after moving the time window by 50 samples. The same time shifting was used to generate the cc maps shown from (c) to (i). Fig. 3 (f) shows the cc map of the moment right after the seizure occurred. A significant change of connectivity patterns can be observed as compared to those shown from Fig. 3 (a) to (e).

TABLE III
EPILEPSY DETECTION PERFORMANCE WITH DIFFERENT TIME SHIFTS.

Time Shift (No. of Samples)	5	10	25	50	100
Accuracy (%)	89.0	90.5	93.5	93.5	91.0
Precision (%)	100.0	100.0	100.0	100.0	98.0
Recall (%)	78.0	81.0	87.0	87.0	84.0

Table III lists the accuracy, precision and recall rates calculated from the epilepsy detection results when five different time shifts were used to form successive EEG data segments. A small time shift means a large overlap of data samples between the successive segments, which share more common functional variations. A shift of 100 samples means no overlap between successive segments, which could generate greater variations in connectivity patterns. The highest accuracy and recall rates are obtained when the time shifts are 25 samples and 50 samples. The detection precision is 100% except for the case when there is no overlap between successive segments. The numerical results indicate that a shift about 25 or 50 samples would be an appropriate setting to form successive segments.

TABLE IV
EPILEPTIC SEIZURE CLASSIFICATION RESULTS WITH DIFFERENT TIME SHIFTS.

Time shift (No. of samples)	5	10	25	50	100
Focal Non-Specific Seizure	24	25	23	25	24
Generalized Non-Specific Seizure	25	25	25	25	24
Simple Partial Seizure	23	22	24	24	22
Complex Partial Seizure	18	18	16	20	17
Absence Seizure	3	3	3	3	4
Tonic Seizure	5	6	7	6	8
Tonic Clonic Seizure	3	4	6	3	2
Control	91	93	94	91	92
Overall Accuracy (%)	78.69	80.33	81.15	80.74	79.10

Table IV shows the classification results of seven seizure types and the control group. The total numbers of evaluation trials in different seizure types are provided in Table II, and the same 100 control group trials used in the detection study were also used here. It is observed that the PaHMM performs better for FNSS, GNSS, and SPS than the other seizure types. The PaHMM model learning and classification performance may also be affected by the number of training trials and the number of subjects in each seizure category. If we compare the overall classification accuracy across all seizure types and the control group, the first two highest accuracies are obtained when the time shifts are 25 samples (81.15%) and 50 samples (80.74%). This is consistent to our observation from the epilepsy detection results.

VI. CONCLUSION

In this work, the dynamic modeling of brain cortical functional connectivity was investigated for the detection and classification of epilepsy. Specifically, a simplified dynamic Bayesian network modeling approach, parallel hidden Markov model, was used to characterize dynamic changes of functional connectivity patterns computed from pre-selected ROIs using multisubject epileptic EEG data from the Temple University Hospital EEG Data Corpus. For the epilepsy detection, a PaHMM was trained to classify subjects with and without epilepsy, and an accuracy of 93.5% was obtained with a precision of 100% and a recall rate of 87%. In the epilepsy classification, another PaHMM was trained to classify seven different types of elliptic seizures and an overall accuracy above 81% was achieved. Compared to the epilepsy detection, the classification of seizure types is more challenge due to limited numbers of training data and subjects. But the experimental results show that the the PaHMM is capable of characterizing temporal variations of cortical functional connectivity, and differentiating different seizure types.

REFERENCES

[1] http://www.who.int/en/news-room/fact-sheets/detail/epilepsy.
[2] C.Ferrie, "Preventing misdiagnosis of epilepsy," *Arch Dis Child.*, vol. 91, no. 3, pp. 206–209, 2006.
[3] H. Qu and J. Gotman, "A patient-specific algorithm for the detection of seizure onset in long-term EEG monitoring: Possible use as a warning device," *IEEE Trans Biomed Eng*, vol. 44, no. 2, pp. 0115–122, 1997.
[4] D. Gajic, Z. Djurovic, and et. al., "Classification of EEG signals for detection of epileptic seizures based on wavelets and statistical pattern recognition," *Biomedical Engineering: Applications, Basis and Communications*, vol. 26, no. 2, p. 1450021, 2014.
[5] D. Novák, T. Al-ani, A. Hamam, and L. Lhotská, "Electroencephalogram processing using hidden Markov models," in *Proc. 5th EUROSIM Congress on Modelling and Simulation*, January 2004, pp. 1–6.
[6] T. Rukat, A. Baker, A. Quinn, and M. Woolrich, "Resting state brain networks from EEG: hidden Markov states vs. classical microstates," arXiv:1606.02344.
[7] M. Fox and M. Raichle, "Spontaneous fluctuations in brain activity observed with functional magnetic resonance imaging," *Nat Rev Neurosci*, vol. 8, pp. 700–711, 2007.
[8] R. Hutchison, T. Womelsdorf, and et. al., "Dynamic functional connectivity:promise, issues, and interpretations," *NeuroImage*, vol. 80, pp. 360–378, 2013.
[9] C. Bielza and P. L. naga, "Bayesian networks in neuroscience: a survey," *Frontiers in Computational Neuroscience*, vol. 8, p. 131, 2014.
[10] J. Rajapakse and J. Zhou, "Learning effective brain connectivity with dynamic bayesian networks," *NeuroImage*, vol. 37, pp. 749–760, 2007.
[11] C. Vogler and D. Metaxas, "A framework for recognizing the simultaneous aspects of American sign language," *Computer Vision and Image Understanding*, vol. 81, pp. 358–384, 2001.
[12] I. Obeid and J. Picone, "The Temple university hospital EEG data corpus," *Frontiers in Neuroscience*, vol. 10, p. 196, 2016.
[13] K. Murphy, "Dynamic bayesian networks: Representation, inference and learning," Ph.D. dissertation, University of California at Berkeley, 2002.
[14] J. Li, Z. Wang, S. Palmer, and M. McKeown, "Dynamic Bayesian network modeling of fMRI: a comparison of group-analysis methods," *NeuroImage*, vol. 41, pp. 398–407, 2008.
[15] J. Vrbik, "Population moments of sampling distributions," *Computational Statistics*, vol. 20, no. 4, pp. 611–621, 2005.